From: FRACTURE MECHANICS OF CERAMICS, Vol. 5
Edited by R. C. Bradt, A. G. Evans, D. P. H. Hasselman, and F. F. Lange
(Plenum Publishing Corporation, 1983)

THE INDENTATION CRACK AS A MODEL SURFACE FLAW

Brian R. Lawn

Department of Applied Physics
University of New South Wales
Kensington, N.S.W. 2033, Australia

ABSTRACT

Recent developments in sharp-indenter fracture techniques for the controlled study of strength-related properties of ceramics and glasses are reviewed. The mechanics of "radial—median" crack evolution are first outlined, thereby establishing the base for a model surface flaw. The response of such cracks to subsequent tensile loading is then described. A key point in the analysis is the vital role played by residual contact stresses in the radial crack growth to failure. Major consideration is given to applications in two areas of strength analysis: flaw characterization and materials evaluation. For the first, surface-stress states associated with multiple-contact processes (e.g. machining), mirror fractography and flaw detection by acoustic wave scattering are topics in which residual-stress effects are manifest. For the second area, the use of indentation flaws for determining basic fracture parameters, such as toughness K_c and crack-velocity exponent n, is given special emphasis. The implications of the results in relation to the design of ceramics for prospective strength-degrading service conditions, particularly in the context of fatigue behavior, are indicated.

1. INTRODUCTION

The underlying basis of all theories of the strength of brittle ceramics derives from the Griffith flaw concept.[1,2] In terms of modern fracture mechanics notation this concept may be embodied in the simple expression $K \sim \sigma_a c^{1/2}$, where σ_a is an applied tensile

stress (assumed uniform over the crack area), c is a characteristic flaw dimension and K is the so-called stress intensity factor. So widely accepted is this basic equation that explicit mention of it tends to be omitted altogether from most current presentations of strength theory in the scientific literature, even in critical review articles. Under *equilibrium* conditions of fracture (approximated with tests in inert environments, high stress rates, low temperatures) the flaw propagates spontaneously to failure when the stress intensity factor reaches a critical value K_c, which defines the material "toughness"; this critical configuration obtains when the applied stress reaches $\sigma \sim K_c/c^{1/2}$, the "inert strength". If fracture occurs under *kinetic* conditions (stress-enhanced crack growth at $K < K_c$, most notably due to interactions with the chemical environment) the flaw grows subcritically from its initial size to some expanded configuration where the requisite condition for failure, $K = K_c$, is once more attained; in combination with some specifiable crack velocity function $v = v(K)$ for the given material—environment system, the basic stress intensity factor equation leads to a relation for the "fatigue strength" in terms of "lifetime" (or some equivalent quantity), with the initial value of c appearing as a controlling crack-size variable. A general conclusion to be drawn from the Griffith hypothesis is that strength is a measure of both intrinsic (material or material—environment) and extrinsic (flaw) parameters.

It is as a direct consequence of this dependence on extrinsic as well as intrinsic parameters that strength data tend to a high degree of scatter; the "typical" flaw is subject to considerable variability in effective size. Since it is usually not possible to locate and observe the critical flaw prior to failure (the *density* of flaws being large, and the *size* small), a priori predictions of strength are not easily made. It is this problem, of course, which has led to the proliferation of statistically-based theories of strength. Unfortunately, while of considerable use for design purposes, the probabilistic approach offers little physical insight into actual flaw processes. A large scatter in data also makes it difficult to evaluate the role of material properties in the characterization of strength. It is in the context of this tendency to variability that the notion of a "controlled" flaw, whose dimensions and location can be accurately predetermined and whose evolution can be followed directly at all stages of testing, presents itself as an attractive alternative route to strength analysis.

Several possible ways of introducing controlled flaws for strength testing have been investigated (including the time-honored method of surface abrasion[3]). Of these, indentation with a sharp, fixed-profile diamond pyramid (Vickers or Knoop) has emerged as the most practical, requiring only access to a routine hardness-testing facility.[4-20] The indentation flaw is character-

ized by a well-defined geometrical pattern and can be accurately positioned on any prospective test surface. Most important, its scale is readily controlled to a high degree of reproducibility, via the contact load. A vital element of the sharp-indenter pattern is the central zone of irreversible ("plastic") deformation about the immediate contact area which accommodates the familiar hardness impression.[21-34] The complex elastic—plastic stresses both generate the microcrack nuclei and drive the ensuing crack segments outward into the final flaw configuration. Central to the theme of this article is the essential role played by the residual component of the elastic—plastic field in the crack evolution:[34] the radial traces of the flaw system are observed to expand outward from the deformation zone as the indenter is *unloaded*, and, indeed, to continue in this expansion long after the contact cycle has been completed.[32] It follows that this residual-contact component must augment the crack driving force provided by the applied tensile field during testing to failure.[24,25,30,33] If this behavior is representative of naturally occurring flaws, and there is growing evidence that it is, then the simplistic Griffith concept of the ideal (residual-stress-free) flaw needs to be re-examined.

Essentially two approaches have been taken in attempts to handle this apparent complication in the indentation-flaw mechanics. The first treats the residual-stress term as a "correction factor", a term preferably eliminated by physical means (e.g. by polishing away or annealing the source of the residual stresses, the central deformation zone).[19] This approach has major limitations: the magnitude of the effect is not easily computed from first principles, and ignoring it can lead to systematic errors of more than a factor of two in strength values; on the other hand, any attempt at physical removal (quite apart from the extra demands on specimen preparation) runs the risk of changing the nature of the flaw, or indeed of the specimen material itself. The second approach is to "learn to live" with the residual-stress effect by incorporating it explicitly into the failure mechanics.[30,33] Although the mathematical treatment is necessarily more detailed the gains in experimental convenience are significant, thereby increasing the viability of the technique as a tool for routine fracture analysis. One of the interesting consequences of the modified theoretical formulation is that the initial crack size no longer appears as a controlling variable - the argument for adopting a statistical view of strength is therefore ineffectual in the case of controlled indentation flaws. As with the first approach, it is acknowledged that absolute predetermination of the residual-stress term is not feasible, so the method requires some "calibration".

Our aim in this article is to review the basic principles of the indentation flaw mechanics, with due attention to the departures from the Griffith flaw concept alluded to above, and to demonstrate how these principles may be used to investigate the strength

properties of ceramics. Two main areas of application will be described; flaw analysis, and materials evaluation. Our focus here will be on more recent developments in the field, without in an way attempting an exhaustive coverage of topics.

2. FRACTURE MECHANICS OF RADIAL CRACK SYSTEM

We consider the indentation flaw system shown schematically in Figure 1. The pattern geometry in this case is that produced by a Vickers diamond pyramid, which is chosen as our standard indenter because of its general facility for providing quantitative information on both deformation and fracture properties from surface measurements alone. Once formed, the indentation flaw is subjected to an applied tensile stress which is to take the system to failure. In this section we set out to summarize the mechanics of the crack evolution, taking the indentation and tensile loading stages separately. Implicit in the analysis will be the assumption that the test material is isotropic, homogeneous, and free of pre-existing stresses.

2.1 Formation of the Radial Crack System

When the sharp indenter contacts the specimen surface it deforms the underlying material irreversibly. The deformed volume is usually referred to as the "plastic zone", although the actual deformation processes may involve other modes such as viscous flow and densification. Empirically, it is found that the characteristic in-surface dimensions of the resultant impression, such as the half-diagonal a in Fig. 1, remain a reasonably faithful indicator of the contact at maximum loading, thus justifying the use of post-indentation measurements to quantify the resistance to deformation. In this way we may define the material "hardness" in terms of the mean contact pressure,

$$H = P/2a^2 \tag{1}$$

where P is the peak contact load. On the other hand, the *depth* of the impression shows a strong recovery in most materials, indicating that the contact mechanics contain an elastic as well as a plastic component. An analysis of the indentation load—unload cycle does in fact show that the degree of depth recovery is determined by the ratio of hardness to Young's modulus, H/E.[35] Since the recovery is never complete except in extraordinary circumstances (e.g. in rubbery materials) it follows that there must exist a state of residual stress about the contact site. Arguing on the basis that the volume of the impression must be accommodated by the elastic matrix surrounding the plastic zone,[34] it can be seen that the associated stress field will be basically radial-compressive and tangential-tensile, much as for an expanding cavity model.

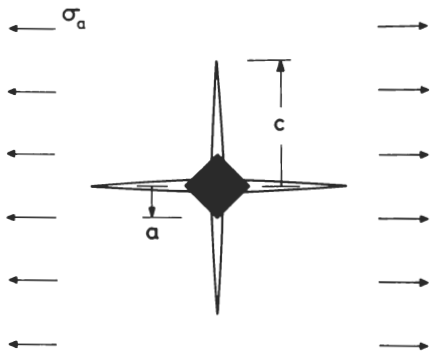

Figure 1. Schematic of Vickers indentation pattern on brittle surface, showing characteristic fracture and deformation dimensions. Radial crack system is subjected to subsequently applied tensile stresses, thereby leading to failure.

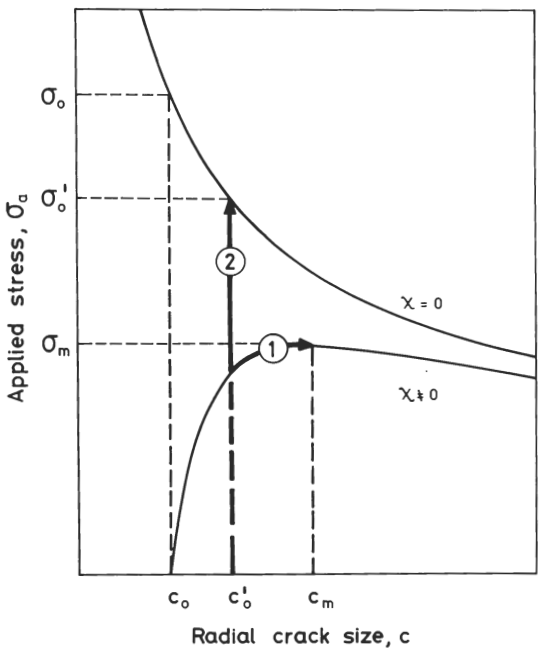

Figure 2. Plot of function $\sigma_a(c)$ in Eqn. 5 for radial cracks with and without residual contact stresses. Curves 1 and 2 indicate respective paths to failure under equilibrium fracture conditions.

Within the deformation zone crack nuclei are generated by the highly disruptive processes of structural rearrangement, and above some threshold contact load these nuclei become critical and propagate into the crack configuration depicted in Fig. 1.[27] The resulting, so-called "median—radial" cracks are of half-penny geometry, contained on two orthogonal median planes each of which passes through the load axis and an impression diagonal, and intersecting the specimen surface to produce the characteristic radial traces. (A second, "lateral" system of cracks generally develops as well, but these cracks are not usually strength-controlling and are accordingly given only minor consideration here.) The actual development of the median—radial cracks (hereafter referred to simply as "radial" cracks) is complex.[34] During the contact the reversible component of the field is actually compressive in the surface regions, and thereby acts as a constraint on radial crack expansion. It is the irreversible component, with its tangentially-directed tensile stresses, which drives the cracks outward as the elastic constraint is released (i.e. as the indenter is unloaded). Accordingly, the fully developed indentation flaw is subject to a persisting crack driving force which, for penny-like configurations, is described by a residual stress intensity factor[32,34]

$$K_P = \chi P/c^{3/2}, \tag{2}$$

where χ is an elastic—plastic parameter which varies approximately as $(E/H)^{1/2}$ for different materials.[34]

If the radial crack system were to persist in equilibrium after completion of the contact cycle, i.e. such that the requirement $K_P = K_c$ were to remain satisfied, then the flaw size prior to strength testing would be given by $c_0 = (\chi P/K_c)^{2/3}$. However, in practise the system is almost invariably exposed to a non-inert environment between the two stages of testing, in which case the flaw extends subcritically to some non-equilibrium size $c_0' > c_0$.[32] (Another potential contributing factor to departure from an equilibrium configuration is relief of the residual stress field, as for instance due to lateral-crack chipping around the plastic zone, causing a reduction in χ.[36]) The final state of the crack system defines the initial conditions for the ensuing strength test.

2.2 Failure of the Radial Crack System in Tensile Loading

Now let us consider how the radial crack system responds to an applied tensile stress σ_a which is ultimately to cause failure. It is assumed that at least one of the median planes is oriented normal to the tensile direction. (In a biaxial test both median planes will, of course, automatically satisfy this requirement.) The stress intensity factor appropriate to this form of loading is of the standard form indicated earlier (Sect. 1),

$$K_\sigma = \psi\sigma_a c^{1/2} \tag{3}$$

where ψ is a crack-geometry parameter (equal to $2/\pi^{1/2}$ for an ideal penny crack without interaction effects from specimen free surface, plastic deformation zone, or adjacent radial or lateral segments). Therefore, the *net* stress intensity factor for the indentation flaw is the sum of K_P and K_σ, i.e.

$$K = \chi P/c^{3/2} + \psi\sigma_a c^{1/2} \qquad (c \geqslant c_0') \cdot \tag{4}$$

This expression represents our generalization of the Griffith flaw concept.

Under conditions of equilibrium fracture ($K = K_c$) we may solve for applied stress as a function of crack size,[30,33]

$$\sigma_a = (K_c/\psi c^{1/2})(1 - \chi P/K_c c^{3/2}) \qquad (c \geqslant c_0') \tag{5}$$

which passes through a maximum at

$$\sigma_m = 3K_c/4\psi c_m^{1/2} \tag{6a}$$

$$c_m = (4\chi P/K_c)^{2/3}. \tag{6b}$$

A plot of the function $\sigma_a(c)$ is shown in Fig. 2 for nonzero and zero χ. For a starting crack of size c_0' the two cases represented have totally different failure paths. Path 1 is distinguished by a stage of precursor radial expansion, from c_0' to c_m, prior to the system reaching an instability at $\sigma_a = \sigma_m$, which defines the appropriate inert strength. Path 2 is the more familiar Griffith limit, where failure occurs at $\sigma_a = \sigma_0' = K_c/\psi c_0'^{1/2}$ without any such stage of precursor growth. It is to be noted that, for all $c_0' < c_m$, we have $\sigma_0' > \sigma_m$ always, consistent with results from comparative strength tests on indented materials with and without the source of residual contact stresses removed;[19,24,30,33] typically, the presence of the residual field reduces the strength by 30-40%, although it is evident from Fig. 2 that this reduction could exceed 100% (at the lower limit of initial crack size, $c_0' = c_0$) under favorable circumstances.

The feature of this description which appeals in the context of strength testing is the insensitivity of the instability configuration defined by Eqn. 6 to initial crack size, *provided* $c_0' < c_m$. This eliminates the need for any direct measurement of crack dimensions (although in some instances such measurements can provide useful "calibrations", as we shall indicate in later sections); rather, the critical stress σ_m is controlled (for any given material) by the contact load P. The essential criterion for determining whether Eqn. 9 is indeed applicable is that the radial crack should,

under inert conditions, show some precursor growth prior to failure. Evidence is accumulating, from direct observations of the crack evolution under stress in glass,[33] silicon,[36] and in several ceramics,[37,38] to suggest that the necessary proviso is in fact almost universally satisfied under normal indentation conditions. Whether or not similar effects are manifest in naturally occurring flaws will depend, of course, on the many factors which characterize the history of the material, as reflected in the value of the χ parameter.

3. FLAW CHARACTERIZATION

The radial crack is ideally suited as a model system for investigating the mechanical response of flaws under different conditions of testing. In this section we shall examine just three topics which illustrate the scope of the method. These examples will serve also to reinforce the need to consider residual-stress terms in the failure mechanics.

3.1 Surface-Stress States Associated With Machining Damage

One of the useful applications of the indentation flaw method which has received some attention is the evaluation of surface stress states.[13,14,18,33,39,40] The motivation for this work comes from the proposal that brittle solids can be significantly strengthened by putting their surfaces into compression. Closure forces then act on the surface flaws, and any subsequent tensile loading must first negate these forces before becoming effective in driving the system toward failure. Provided the compressive stress is uniform over the crack area, determination of its magnitude is reasonably straightforward, for under such circumstances the principles of stress superposition prevail; the requisite value is determined from tests on as-indented specimens as the difference in strength between treated and untreated (stress-free control) surfaces.[33] If the stress distribution is non-uniform, however, i.e. if the compressive layer is not large compared with the depth of the flaws, the evaluation is far more complex.[41,42]

With this background, we may examine some recent results obtained on a glass-ceramic, Pyroceram C9606 (Corning), which bear strongly on the mechanics of flaw growth.[43] Bars in suitable form for bend testing were indented at a prescribed load, and their strengths duly measured under inert testing conditions. The results were found to be sensitive to surface finish: bars whose surfaces had been heavily machined (400-mesh diamond-grit wheel) were stronger, by as much as 50%, than bars with polished surfaces (down to 1 μm diamond paste). Closer examination of this effect was made by polishing away portions of the damage layer on the machined surfaces prior to indentation, so that the as-indented strength

could be followed systematically as a function of the depth removed. The data are plotted in Fig. 3. Notwithstanding the scatter in points, the trend is clear - since the indentation conditions are invariant, the surface polishing must be progressively removing a crack-closure force associated with the machining damage. This conclusion is consistent with our previous picture of the elastic—plastic stress field about individual indentation centers (Sect. 2.1): although a specific median-plane crack segment will experience the tangential component (tensile) from its own deformation zone, it will experience the radial component (compressive) from any neighbors; thus, if we can regard the machining process as the cumulative end result of a high density of such "indentation events", the net effect of the surrounding damage layer on the flaw which is ultimately to cause failure will be one of crack closure.

Of course, apart from introducing a surface-compressive state, the machining process introduces its own cracks. According to the above interpretation, these cracks will be expected to respond in much the same way as the radial-crack system. The major advantage of the indentation technique in these experiments is that the machining compressive layer can be systematically removed without affecting the constancy of the dominant flaw; if the specimens were allowed to fail from the machining cracks themselves the strength decrease evident in Fig. 3 would tend to be obscured by a trend of opposite sign due to an attendant reduction in the flaw size. A more detailed investigation of the machining-damage phenomenon than we are able to cover here indicates that the compressive stress is unlikely to be uniformly distributed over the crack depth, making quantitative analysis difficult.[43] It is nevertheless clear from Fig. 3 that the scale of the effect can be substantial, and is not to be ignored in any proper treatment of flaw response for surfaces with heavy damage layers.

3.2 Mirror Surface Fractography

Useful information on the mechanical characterization of a critical flaw which has caused component failure can be gained from a microscopic examination of the fracture faces. With brittle solids it is found that the fracture origin at the critical flaw is marked by a surrounding, well-defined morphological pattern, loosely termed the fracture "mirror". The mirror region is generally smooth, and is itself surrounded by increasingly rougher regions known as "mist" and "hackle". The pattern has approximate radial symmetry about the flaw origin. Figure 4 shows the main features. The importance of the mirror pattern lies in the fact that it tends to scale with the flaw size, thereby providing a means of quantitative analysis (for reviews, see Refs. 44 and 45). This result is particularly useful where the initial flaw is too small or ill-defined for conventional microscopic observation.

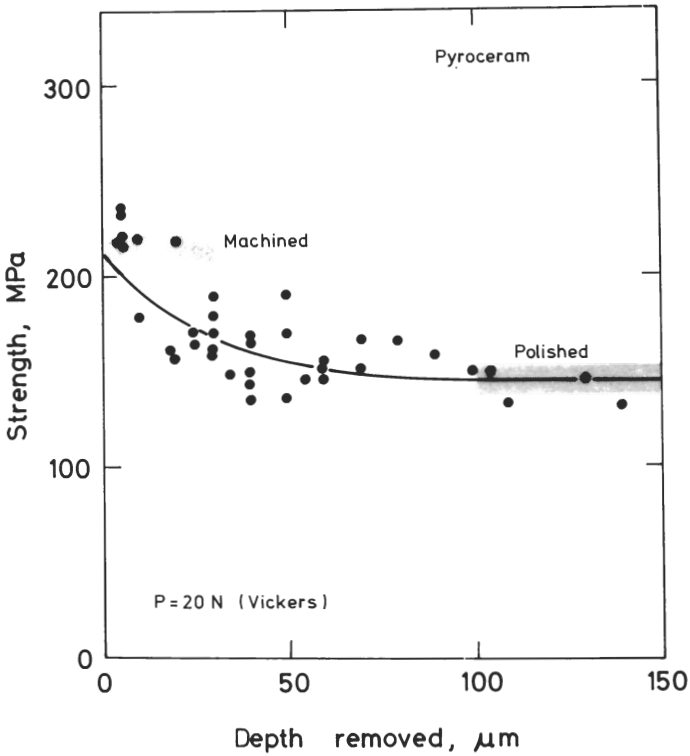

Figure 3. Variation of inert strength for as-indented glass-ceramic surfaces containing machining damage, as function of depth of material removed.

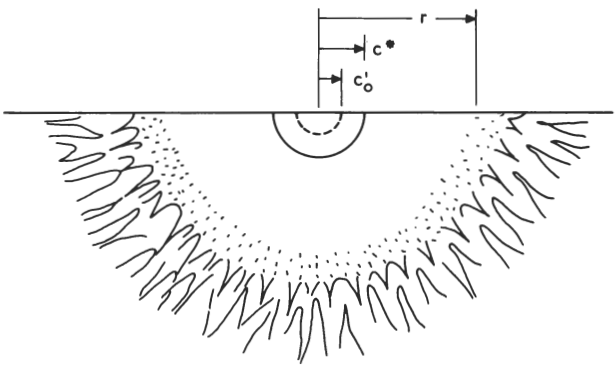

Figure 4. Schematic of mirror zone about indentation flaw.

Again, in setting up a fracture mechanics formalism to describe the mirror phenomenology, it is important to pay attention to the starting equation for the crack driving force. Most treatments begin, in the usual manner, with the assumption of an ideal Griffith flaw. However, in the general case the flaw will be influenced in its growth by a residual-stress component, in which event a relation akin to Eqn. 4 should be used. On the assumption that the mirror delineates the zone between $c = c^*$, where the flaw becomes critical at $K = K_c$, and $c = r$, where the stress intensity attains a level $K = K_r$ sufficiently great to induce crack-plane instabilities (thence generating the mist and hackle markings), we may conveniently demonstrate this residual-stress influence by considering the cases of zero and nonzero χ in Eqn. 4. We take these two cases separately, restricting our discussion to inert testing conditions:

(i) Zero residual term. For $\chi = 0$, failure occurs at $\sigma_a = \sigma_0'$ (path 2 in Fig. 2), whence Eqn. 4 yields $c^* = c_0' = (K_c/\psi\sigma_0')^2$ at failure and $r = (K_r/\psi\sigma_0')^2$ at the mirror boundary (assuming the stress to remain constant during the post-failure propagation). Thus we obtain the mirror-radius/flaw-size ratio

$$r/c^* = (K_r/K_c)^2 \qquad (\chi = 0). \tag{7}$$

(ii) Nonzero residual term. For $\chi \neq 0$, failure occurs at $\sigma_a = \sigma_m$ (path 1 in Fig. 2), so we have $c^* = c_m = (3K_c/4\psi\sigma_m)^2$ at failure (see Eqn. 6a) and $r \simeq (K_r/\psi\sigma_m)^2$ at the mirror boundary (from Eqn. 4, in the approximation $r >> c^*$, where the residual term can be neglected). The mirror/flaw ratio is

$$r/c^* = (4K_r/3K_c)^2 \qquad (\chi \neq 0) \tag{8}$$

which is a factor of 1.78 greater than the corresponding ratio in Eqn. 7.

The above formulation has been tested on Vickers-indented soda-lime glass specimens.[46] In these tests some specimens were broken in their as-indented state ($\chi \neq 0$), and some after a post-indentation anneal ($\chi = 0$). The r/c^* values obtained from the two sets of specimens were 9.0 and 5.0 respectively, corresponding to a factor of 1.80, in support of the theoretical prediction. It is apparent that the mirror/flaw ratios are far from universally constant quantities, and that due care must be taken to establish the nature of all fracture driving forces before using mirror dimensions to ascertain flaw sizes. In this context Mecholsky has recently shown in tests on machined surfaces that grinding flaws are subject to the same kind of discrepancy as described here for controlled indentation systems.[47]

3.3 Acoustic Detection of Flaws

Mirror fractography is necessarily restrictive as a diagnostic tool in failure analysis because it can only provide information *after* the event. An altogether different methodology which is currently of intense interest for its potential use as a means of characterizing critical flaws *before* failure is that which involves acoustic sensors. The approach has many variants, but all are based on the principle that cracks can interact effectively (either by absorption, reflection or emission) with elastic waves. In this section we shall concern ourselves with one such variant which monitors back-scattered Rayleigh (surface) waves initially incident normally onto the plane of a well-defined indentation flaw.[48]

Results of tests using this technique on Knoop-indented, polished silicon nitride (NC 132; Norton) are shown in Fig. 5.[49] (The Knoop indenter produces a *single* radial crack segment, which is the simplest configuration for acoustic scattering analysis.) The diagram indicates how an applied tensile stress acting across the crack plane affects the acoustic response, for both as-indented ($\chi \neq 0$) and post-indentation-annealed ($\chi = 0$) specimens. It can be demonstrated that the scattering efficiency for Rayleigh waves is a measure of the displacement discontinuity integrated over the crack area, in which case we may immediately attribute the reduced signal for the annealed flaw at zero applied stress to the removal of a residual-contact opening displacement. The interpretation of the relative signal strengths once loading has begun is not so straightforward, however, for enhancement can come from increases in either the crack-wall separation or the crack area. Distinction between these two contributing factors can be made by judiciously unloading and reloading the specimens during the tests to failure, in the manner shown in Fig. 5, and arguing that the first factor should be reversible, the second not. (Reversibility in crack extension *can* occur, but only in exceptional circumstances, and even then only partially - see Ref. 50.) Thus we may conclude from the two curves in Fig. 5 that significant precursor stable crack extension has occurred in the as-indented specimen, but not in the annealed specimen, again consistent with the fracture mechanics description of Sect. 2.2.

Although the results in Fig. 5 represent measurements made on just two specimens in an as-yet incomplete program of study,[49] they carry strong implications in the context of non-destructive testing. It is clear that the best conditions for detecting the prospective onset of failure obtain where the flaws are subject to a residual-stress effect, i.e. with the specimens in their "as-indented" state. (Of course, annealing *after* testing may be recommended as a means of strengthening components prior to service, thereby providing a safety margin in design specifications.) Preliminary tests have

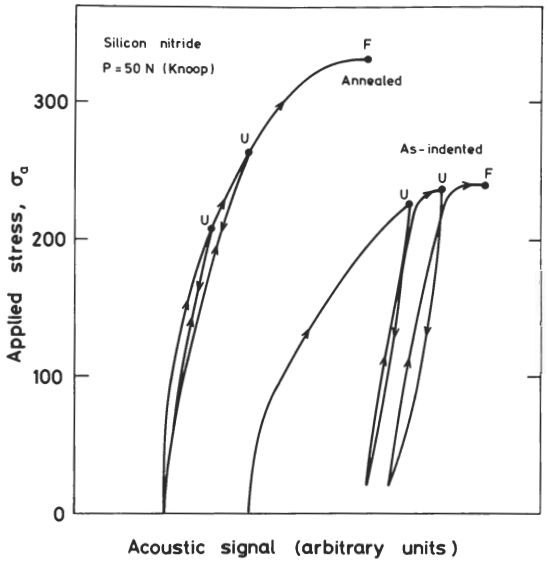

Figure 5. Showing stress—signal variations for backscattered Rayleigh waves (8.5 MHz) on indented, polished surfaces. *U* designates unload point, *F* failure. Note that significant hysteresis occurs on the as-indented specimen, but not on the (post-indentation) annealed specimen. (Courtesy J.J.W. Tien, B.T. Khuri-Yakub, G.S. Kino, D.B. Marshall, A.G. Evans.)

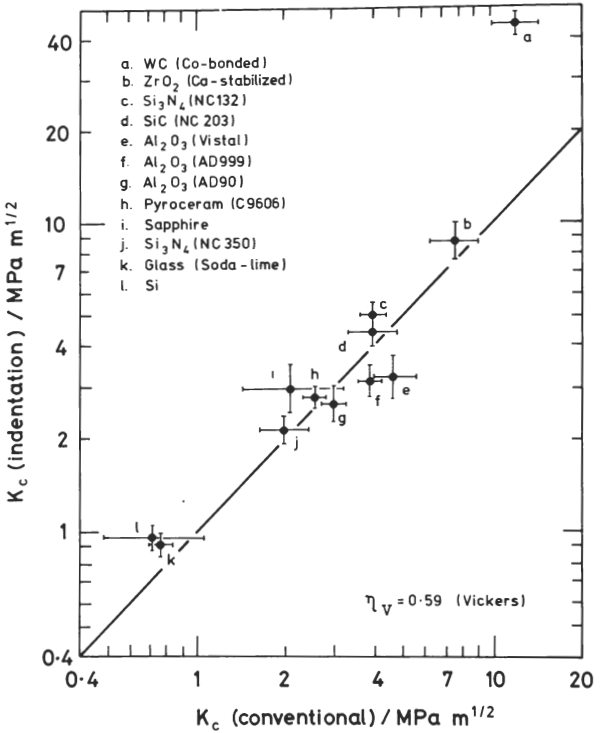

Figure 6. Plot showing correlation between toughness values determined for various ceramics. Vertical error bars are standard deviations, horizontal error bars are nominal uncertainty levels.

also been made on as-machined surfaces,[51] and apparently exhibit the same kind of unload—reload response as the as-indented surface in Fig. 5, reinforcing yet again the contention that the typical flaw in ceramics may be far removed from the Griffith idealization.

4. MATERIALS EVALUATION

The indentation method produces a crack system which satisfies all the essential requirements of a controlled flaw in the evaluation of material fracture parameters. As we have seen, the strength of as-indented specimens is insensitive to any factors which might be expected to influence the initial crack size, provided $c_0' < c_m$; it is the crack size c_m which emerges as the key dimension in the failure mechanics, and for any given material this quantity is uniquely determined by the contact load (Eqn. 6b). We describe here how this element of control can be put to use in evaluating materials under both equilibrium and fatigue conditions of fracture.

4.1 Toughness Parameters

There have been several attempts to measure the toughness parameter K_c (or some equivalent quantity, such as fracture surface energy) in ceramics from direct observations of radial crack dimensions.[52–55] However, these attempts all derive from somewhat phenomenological treatments of the indentation fracture mechanics, and tend to overlook the vital role of the inelastic component of the contact field. Thus, for instance, it has not widely been appreciated that post-indentation crack extension can be substantial in some materials, in which case the scale of the indentation pattern no longer represents an equilibrium state. One could in fact make use of the crack-evolution description of Sect. 2.1 to modify the earlier treatments, taking Eqn. 2 as the basis for evaluating the critical stress intensity factor at completion of the contact cycle. Nevertheless, as shown in a recent critical study of this approach,[56] there are certain limitations which inevitably attend any procedure that relies directly on measurement of small-scale crack dimensions.

Many of these implied limitations can be circumvented by using the formulation of Sect. 2.2 to relate toughness to the strength of as-indented specimens. Accordingly, recalling from Sect. 1 that $\psi \sim (E/H)^{1/2}$, we may rearrange Eqn. 6 to obtain, pertinent to inert testing environments,

$$K_c = \eta (E/H)^{1/8} (\sigma_m P^{1/3})^{3/4} \tag{9}$$

where η is a material-independent constant for a given indenter. Hence, given the modulus/hardness ratio (which clearly need not be known to high accuracy) and an appropriate "calibration" of η,

toughness is determined by the two readily measurable indentation—strength load variables, P and σ_m. The absence of initial crack size c_0' in Eqn. 9 is now seen as a major advantage; there is no need for any direct observation of the crack system (other than to confirm that it is well-behaved). A detailed study of this alternative approach has been conducted on a range of Vickers-indented ceramics,[57] using independent toughness determinations on conventional test-pieces (double torsion) to obtain an appropriate Vickers constant η_V in Eqn. 9. The values of K_c thus computed from the indentation—strength formulation are plotted in Fig. 6 against those measured independently. There is evidence of some systematic discrepancies in the correlation (notably for tungsten carbide), most of which appear to be connected with departures from the idealized radial-crack geometry.[57] On the other hand, it can be argued that the indentation-determined toughness for such less well-behaved materials, while perhaps not truly representative of macroscopic crack propagation, may nevertheless be more appropriate to the description of fracture properties at the flaw level.

The indentation—strength method lends itself to the systematic investigation of fracture toughness *variations*, for example due to changes in material composition, grain size, stress rate or temperature. As an illustration, we consider briefly the results of studies by two groups of workers on the functional variation $K_c(T)$ in ceramics[16,17] and glasses.[58] The first of these groups ran tests on as-indented surfaces of a lithium-aluminium-silicate glass-ceramic[16] and a silicon nitride,[17] and found the fracture strength to remain reasonably steady up to a certain temperature in each material, above which the strength rose rapidly, peaked, and then declined. The rapid rise was attributed to "crack blunting" due to viscosity effects associated with glassy phases at the grain boundaries. The same workers acknowledged that a similar rise might be produced by annealing of the residual contact stresses, but presumed this effect to be of negligible proportions in their materials. In view of the consistently large residual-stress effects reported earlier here (Sect. 2) and elsewhere for similar materials, it would appear that this interpretation requires more definitive evidence. The distinction between the two possible mechanisms is relevant to the evaluation of toughness characteristics, in that the first mechanism represents a true increase in K_c, whereas the second does not. This complication was avoided altogether by the second group of workers, who annealed their indented glass specimens prior to strength testing.[58] In this case the onset of elevated-temperature viscosity effects in the toughness parameter could be identified without ambiguity. The results of these two studies serve to re-emphasize the need for complete characterization of the critical flaw. As pointed out in Sect. 1 the approach which seeks to remove the residual-stress term by physical means, as adopted here by the second group of workers, is not always practical; some attention should therefore be given to establishing the magnitude of the

residual-stress contribution wherever ambiguity might possibly arise. Thus the issue referred to above might be resolved by examining the reversibility of the room-temperature strength after passing the indentation flaw through an appropriate thermal cycle, taking special care to "re-sharpen" the cycled cracks.[33]

4.2 Crack Velocity Parameters

Perhaps the area of materials evaluation which stands to gain most from the application of controlled-flaw techniques is that of fatigue testing. Room temperature fatigue failure in ceramics is now recognized as a subcritical, rate-dependent crack growth phenomenon, governed by some stress-dependent crack velocity function $v = v(K)$. The origins of this function are rooted in the kinetics of crack-tip chemistry. Its most widely used form is

$$v = v_0 (K/K_c)^n \qquad (K < K_c) \tag{10}$$

where v_0 and n are kinetic constants for a given material—environment system. (For a critical discussion of the various alternative forms proposed for $v(K)$ see Ref. 59.) Insertion of an appropriate stress intensity factor $K = K(\sigma_a, c)$ into Eqn. 10 then gives us a starting kinetic equation which, for any specified time variation of applied stress, $\sigma_a = \sigma_a(t)$, reduces to a differential equation for crack size in terms of time. Solution of this differential equation is obtained by integrating between $c = c_0'$ at $t = 0$ and $c = c_f$ (determined explicitly as the critical instability configuration $K(c_f) = K_c$, $dK/dc > 0$) at $t = t_f$. For "static fatigue" the solution t_f defines the lifetime at a given applied stress, σ_a = const.; for "dynamic fatigue" the solution defines the fatigue strength $\sigma = \sigma_a(t_f) = \dot{\sigma}_a t_f$ at a given stress rate, $\dot{\sigma}_a$ = const.

In terms of the indentation flaw system described in Sect. 2 the appropriate stress intensity factor for insertion into the crack velocity function is given by Eqn. 4. Our differential equation therefore becomes

$$\dot{c}/v_0 = \{(\chi/K_c)P/c^{3/2} + (\psi/K_c)\sigma_a c^{1/2}\}^n. \tag{11}$$

Definitive confirmation of this formulation has been obtained in these laboratories from dynamic[60] and static[61] fatigue studies on soda-lime glass in water. In these studies, specimens were tested both as-indented and post-indentation-annealed (taking care in the latter case to re-sharpen the radial cracks). Results from the static fatigue study are shown in Fig. 7. It is immediately apparent that the presence of the residual-stress component has a substantial influence on the specimen lifetimes, the more so at the lower stress levels. The curves through the two sets of data points in this figure were generated from Eqn. 11 in accordance with the following parameter calibration procedure: (i) measure initial

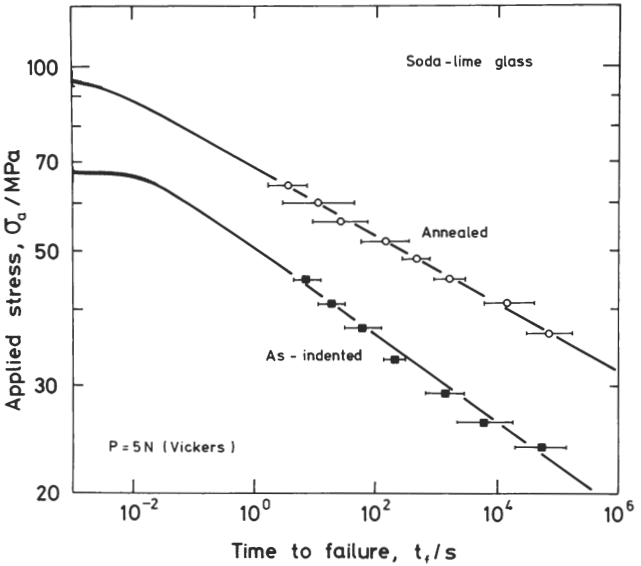

Figure 7. Static fatigue results for indented glass surfaces, tested in water. Shaded regions indicate inert strength levels. Error bars on data points are standard deviations. Note substantially shorter lifetimes of as-indented as compared to (post-indentation) annealed specimens.

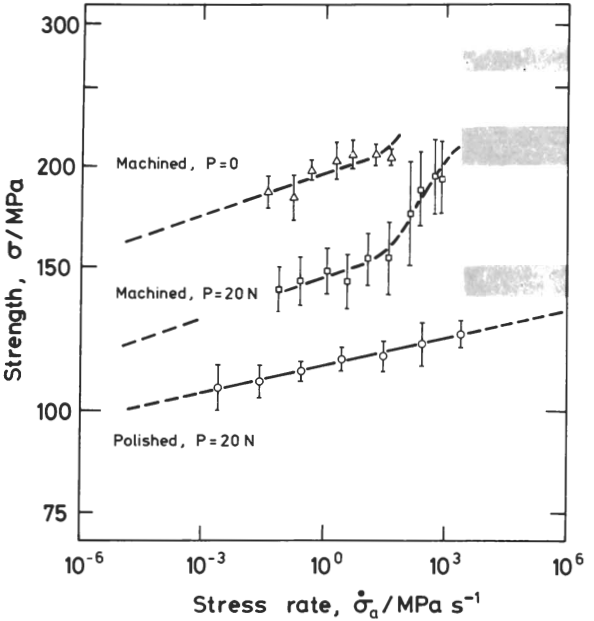

Figure 8. Dynamic fatigue results for Pyroceram glass-ceramic surfaces tested in water. Lower two curves represent Vickers-indented specimens, upper curve (courtesy B.J. Pletka and S.M. Wiederhorn) unindented specimens. Shaded regions indicate appropriate inert strength levels. Error bars are standard deviations.

radial crack dimension c_0'; (ii) for the annealed specimens ($\chi = 0$), adjust K_c/ψ to match the inert-strength quantity $\sigma_0' c_0'^{1/2}$ (equilibrium solution of Eqn. 5) and v_0 and n to match the data in the fatigue (linear) region; (iii) for the as-indented specimens, adjust K_c/χ to match the inert-strength quantity $\sigma_m P^{1/3}$ (see Eqn. 6, in conjunction with the parameter K_c/ψ just determined). Effectively, this procedure uses a fit to the data for flaws *without* residual stress to predict the corresponding fatigue response for flaws *with* residual stress. The goodness of fit between curve and data points for the as-indented specimens may therefore be taken as a measure of the validity of the indentation theory.

The approach just outlined, based as it is on a comparative analysis of specimens representing limiting cases of the χ term, is hardly a practical proposition for the general fatigue testing of ceramics. We have already mentioned the desirability of obtaining fatigue data on as-indented specimens alone (Sect. 1). It is in this spirit that a generalized theoretical analysis of Eqn. 11 has been developed, explicitly for dynamic fatigue conditions.[62] The analysis shows that by judicious reduction of variables the solutions of Eqn. 11 correspond to a universal fatigue curve determined uniquely by the crack velocity exponent n. Central to the reduced-variable scheme is the critical configuration defined by Eqn. 6: it is seen that by normalizing terms in stress with respect to σ_m, crack size with respect to c_m, and time with respect to c_m/v_0, Eqn. 11 becomes independent of the material—environment—indenter system. Moreover, provided the condition $c_0' < c_m$ is once more respected, the solutions are highly insensitive to c_0' itself, so adoption of c_0 (see Fig. 2) as an invariant initial condition eliminates a potential variable. (Physically, this insensitivity is due to the fact that the minimum in K, which defines the rate-controlling region of crack growth, falls beyond c_m for all $\sigma < \sigma_m$.) When plotted in logarithmic coordinates the curves generated from Eqn. 11 tend to linearity in the fatigue region, in which case we may write, in analogy with the conventional form of the strength—stress-rate relation (i.e. for Griffith-like flaws without residual-contact stresses)

$$\sigma = (\lambda' \dot{\sigma}_a)^{1/(n'+1)} \qquad (\sigma < \sigma_m) \tag{12}$$

where the primes are to indicate that the usual slope and intercept evaluations will yield "apparent" kinetic parameters. Conversion to "true" values is achieved via the "transformation" relations[62]

$$n = 1.31\, n' \tag{13a}$$

$$v_0 = 2.84\, n'^{\,0.462}\, \sigma_m^{n'}\, c_m/\lambda' \tag{13b}$$

derived from analysis of the universal fatigue curves.

To illustrate the application of the above theoretical analysis a case study has been carried out on the same Pyroceram glass-ceramic as used in the machining damage tests described in Sect. 3.1.[63] Bars were Vickers-indented at a prescribed load and then bend tested to failure in water over a range of stress rates. Tests on polished surfaces were used to provide baseline data for detailed analysis (these surfaces being free of precompressive stress layers); tests were also run on machined surfaces, to investigate the effect of such layers on the fatigue characteristics. The results are shown in Fig. 8, together with some others from Ref. 64 on machined surfaces *without* indentations. For the baseline data, the curve represents a theoretical fit of Eqn. 11, evaluated in accordance with the following procedure:

(i) Run inert-strength tests to obtain the key normalization parameters σ_m and c_m. (The latter is most conveniently measured by placing more than one indentation on the test surface, so that "dummy" crack systems remain intact for post-failure examination.[63] This contrivance is also useful for ensuring that the proviso $c_0' < c_m$ is satisfied.) Determine the equilibrium quantities K_c/χ and K_c/ψ from Eqn. 6.

(ii) Perform linear regression analysis of the data in log σ vs log $\dot{\sigma}_a$ to obtain n' and λ'. Then "transform" these quantities using Eqn. 13 (in conjunction with the inert strength parameters already determined) to give n and v_0.

(iii) As a check, regenerate the dynamic fatigue curve from the master differential equation, using the determinations of (i) and (ii) together with the given load P at specified stress rates $\dot{\sigma}_a$. (This exercise should be seen as a test of the accuracy of the transformation equations, and of the validity of several assumptions implicit in the formulation.)

A comparable analysis of the upper two sets of data in Fig. 8 is not considered feasible at this stage because of the complex nature of the precompressive stress layer (Sect. 3.1); we include these extra data simply to highlight yet again the importance of proper flaw characterization in the study of fracture properties (see Ref. 63 for a more complete discussion).

As a second illustration of the technique we plot in Fig. 9 some recent results of a dynamic fatigue study on soda-lime and borosilicate glass rods.[65] The specimens were Vickers-indented in the usual way, but this time with load P used as a test variable. The purpose of this study was to investigate the range of flaw sizes over which macroscopic crack laws might remain valid, with special attention to possible lower limits for meaningful extrapolations. It can be shown, in accordance with the normalization scheme outlined above, that the load variable may be suitably

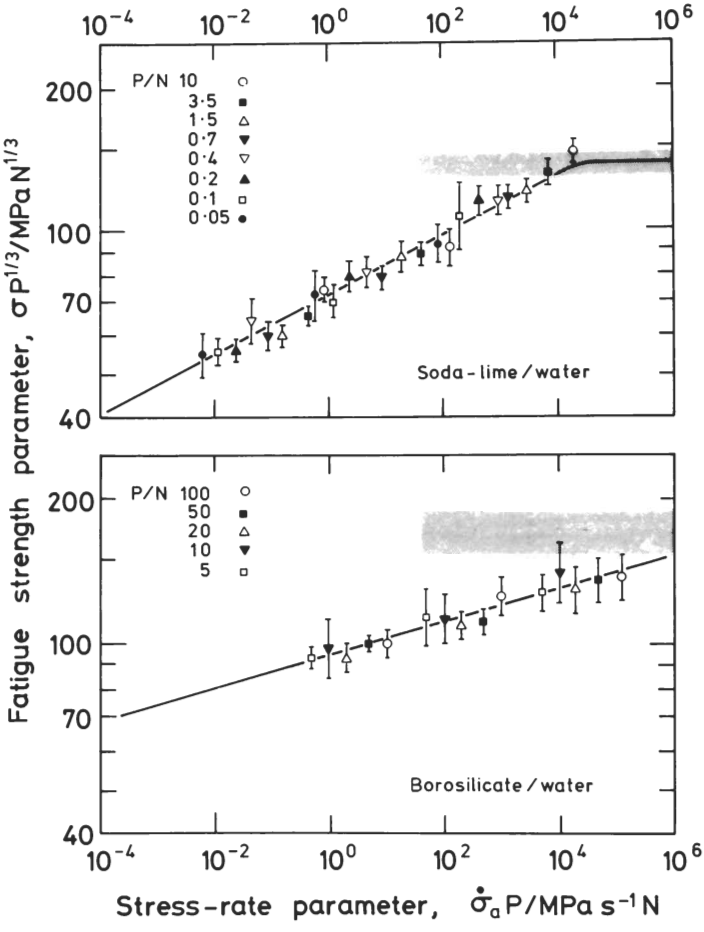

Figure 9. Dynamic fatigue results for as-indented glass surfaces, with variable load P incorporated into coordinates so as to produce universal plots. Shaded regions indicate inert strengths. Error bars are standard deviations.

accommodated in the fatigue plot by taking log $\sigma P^{1/3}$ and log $\dot{\sigma}_a P$ as modified coordinates:[65] any systematic departures from the specified crack laws will then be seen as deviations from universal fatigue curves. Within the confines of experimental scatter, no such deviations are evident in Fig. 9, which represents data down to the thresholds for radial crack formation. (Below the thresholds significant deviations become apparent,[66] which carries special implications for analytical procedures based on extrapolations into the domain of ultra-high strengths, e.g. optical fibers.[67]) The solid curves in the figure again represent theoretical fits of Eqn. 11, using the same sequence of steps as outlined in connection with the Pyroceram data analysis. The values of the crack velocity exponents obtained from the fitting procedure, n = 18.4 (n' = 14.0) for soda-lime and n = 36.4 (n' = 27.8) for borosilicate, are consistent with those generally quoted in the scientific literature.

It is thus clear that the residual-stress term in the fracture mechanics equations can have a profound influence on the fatigue reponse. In terms of materials evaluation it is important to take this term into account, for otherwise the parameters determined may not be representative of true crack growth laws; witness the divergence of the two sets of data in Fig. 7, the slope of the upper curve (χ = 0) measuring n and that of the lower curve ($\chi \neq 0$) measuring n'. "Ordinary" flaws may be expected to lie somewhere within these two extremes of behavior, depending on their mechanical, thermal and chemical history.[68] Insofar as design considerations are concerned, particularly in the prediction of component lifetimes, the distinction between true and apparent fracture parameters takes on a special significance. An extrapolation of results to long lifetimes may be made using either of the parameter evaluations:[61] with apparent values one may proceed without regard to the nature of the flaws, using conventional strength theory as the basis for extending the fatigue curve beyond the practical range of data accumulation,[59] in which case the analysis is totally empirical and the foundation for a wider compass of predictions (e.g. from macroscopic crack laws) is lost; with true values the analysis, albeit somewhat more complex (involving the need to transform the measured parameters, via Eqn. 13), derives from an explicit treatment of the flaw micromechanics, thus preserving all the advantages of self-consistency with well-defined crack laws.

ACKNOWLEDGEMENTS

The author wishes to acknowledge the vital contribution made by D.B. Marshall while at the University of New South Wales, and subsequently at the University of California, Berkeley, to the initial work on the residual-contact effect. Many of the results presented here were obtained in graduate research programs by P. Chantikul, T.P. Dabbs and R.F. Cook.

REFERENCES

1. A.A. Griffith, The phenomena of rupture and flow in solids, *Phil. Trans. Roy. Soc. Lond.* A221: 163 (1920).
2. B.R. Lawn and T.R. Wilshaw, "Fracture of Brittle Solids," Cambridge University Press, London (1975).
3. R.E. Mould and R.D. Southwick, Strength and static fatigue of abraded glass under controlled ambient conditions, *J. Am. Ceram. Soc.* 42: 542, 582 (1959).
4. P. Kenny, The application of fracture mechanics to cemented tungsten carbides, *Powder Met.* 14: 22 (1971).
5. R.K. Govila, Cleavage fracture of VC monocrystals, *Acta Met.* 20: 447 (1972).
6. N. Inglestrom and N. Nordberg, The fracture toughness of cemented tungsten carbides, *Eng. Fract. Mechs.* 6: 597 (1974).
7. K.R. Kinsman, M. Yessik, P. Beardmore and R.K. Govila, On techniques for emplacing small cracks of controlled size in brittle solids, *Metallography* 8: 351 (1975).
8. K.R. Kinsman, R.K. Govila and P. Beardmore, The varied role of plasticity in the fracture of inductile ceramics, p.465 *in* "Deformation of Ceramic Materials," R.C. Bradt and R.E. Tressler, eds., Plenum, New York (1975).
9. J.J. Petrovic, L.A. Jacobson, P.K. Talty and A.K. Vasudevan, Controlled surface flaws in hot-pressed Si_3N_4, *J. Am. Ceram. Soc.* 58: 113 (1975).
10. J.J. Petrovic and L.A. Jacobson, Controlled surface flaws in hot-pressed SiC, *J. Am. Ceram. Soc.* 59: 34 (1976).
11. R.R. Wills, M.G. Mendiratta and J.J. Petrovic, Controlled surface flaw-initiated fracture in reaction-bonded Si_3N_4, *J. Mater. Sci.* 11: 1330 (1976).
12. B.R. Lawn, E.R. Fuller and S.M. Wiederhorn, Strength degradation of brittle surfaces: sharp indenters, *J. Am. Ceram. Soc.* 59: 193 (1976).
13. D.B. Marshall and B.R. Lawn, Strength degradation of thermally tempered glass plates, *J. Am. Ceram. Soc.* 61: 21 (1978).
14. D.B. Marshall, B.R. Lawn, H.P. Kirchner and R.M. Gruver, Contact-induced strength degradation of thermally treated $A\ell_2O_3$, *J. Am. Ceram. Soc.* 61: 271 (1978).
15. B.R. Lawn and D.B. Marshall, Indentation fracture and strength degradation of ceramics, p.205 *in* "Fracture Mechanics of Ceramics," Vol. 3, R.C. Bradt, D.P.H. Hasselman and F.F. Lange, eds., Plenum, New York (1978).
16. R.K. Govila, K.R. Kinsman and P. Beardmore, Fracture phenomenology of a lithium-aluminium-silicate glass-ceramic, *J. Mater. Sci.* 13: 2081 (1978).
17. R.K. Govila, K.R. Kinsman and P. Beardmore, Phenomenology of fracture in hot-pressed silicon nitride, *J. Mater. Sci.* 14: 1095 (1979).
18 P. Chantikul, D.B. Marshall, B.R. Lawn and M.G. Drexhage, Contact-damage resistance of partially leached glasses,

J. Am. Ceram. Soc. 62: 551 (1979).
19. J.J. Petrovic and M.G. Mendiratta, Fracture from controlled surface flaws, p.83 *in* "Fracture Mechanics Applied to Brittle Materials," S.W. Freiman, ed., A.S.T.M. Special Technical Publication 678, Philadelphia (1979).
20. B.R. Lawn, D.B. Marshall, P. Chantikul and G.R. Anstis, Indentation fracture: applications in the assessment of strength of ceramics, *J. Aust. Ceram. Soc.* 16: 4 (1980).
21. B.R. Lawn and M.V. Swain, Microfracture beneath point indentations in brittle solids, *J. Mater. Sci.* 10: 113 (1975).
22. B.R. Lawn and T.R. Wilshaw, Indentation fracture: principles and applications, *J. Mater. Sci.* 10: 1049 (1975).
23. B.R. Lawn, T. Jensen and A. Arora, Brittleness as an indentation size effect, *J. Mater. Sci.* 11: 573 (1976).
24. J.J. Petrovic, R.A. Dirks, L.A. Jacobson and M.G. Mendiratta, Effects of residual stresses on fracture from controlled surface flaws, *J. Am. Ceram. Soc.* 59: 177 (1976).
25. M.V. Swain, A note on the residual stress about a pointed indentation impression in a brittle solid, *J. Mater. Sci.* 11: 2345 (1976).
26. A.G. Evans and T.R. Wilshaw, Quasi-plastic solid particle damage in brittle materials, *Acta Met.* 24: 939 (1976).
27. B.R. Lawn and A.G. Evans, A model for crack initiation in elastic—plastic indentation fields, *J. Mater. Sci.* 12: 2195 (1977).
28. M.V. Swain and J.T. Hagan, The origin of median and lateral cracks at plastic indents in brittle materials, *J. Phys. D.* 11: 2091 (1978).
29. A. Arora, D.B. Marshall, B.R. Lawn and M.V. Swain, Indentation deformation—fracture of normal and anomalous glasses, *J. Non-cryst. Solids* 31: 415 (1979).
30. B.R. Lawn and D.B. Marshall, Residual stress effects in failure from flaws, *J. Am. Ceram. Soc.* 62: 106 (1979).
31. B.R. Lawn and D.B. Marshall, Hardness, toughness and brittleness: an indentation analysis, *J. Am. Ceram. Soc.* 62: 347 (1979).
32. D.B. Marshall and B.R. Lawn, Residual stress effects in sharp contact cracking: I. Indentation fracture mechanics, *J. Mater. Sci.* 14: 2001 (1979).
33. D.B. Marshall, B.R. Lawn and P. Chantikul, Residual stress effects in sharp contact cracking: II. Strength degradation, *J. Mater. Sci.* 14: 2225 (1979).
34. B.R. Lawn, A.G. Evans and D.B. Marshall, Elastic—plastic indentation damage in ceramics: the median—radial crack system, *J. Am. Ceram. Soc.* 63: 574 (1980).
35. B.R. Lawn and V.R. Howes, Elastic recovery at hardness indentations, *J. Mater. Sci.*, in press.
36. B.R. Lawn, D.B. Marshall and P. Chantikul, Mechanics of strength-degrading contact flaws in silicon, *J. Mater. Sci.*, in press.
37. D.B. Marshall, unpublished work.
38. R.F. Cook and B.R. Lawn, unpublished work.

39. B.R. Lawn, D.B. Marshall and S.M. Wiederhorn, Strength degradation of glass impacted with sharp particles: II. Tempered surfaces, *J. Am. Ceram. Soc.* 62: 71 (1979).
40. P. Chantikul, B.R. Lawn and D.B. Marshall, Contact-induced failure of prestressed glass plates, *J. Am. Ceram. Soc.* 62: 340 (1979).
41. B.R. Lawn and D.B. Marshall, Contact fracture resistance of physically and chemically tempered glass plates: a theoretical model, *Phys. Chem. Glasses* 18: 7 (1977).
42. J.T. Hagan, M.V. Swain and J.E. Field, Stress corrosion characteristics of toughened glasses and ceramics, *J. Mater. Sci.* 13: 189 (1978).
43. R.F. Cook, B.R. Lawn, T.P. Dabbs and P. Chantikul, Effect of machining damage on the strength of a glass-ceramic, *Comm. Am. Ceram. Soc.*, in press.
44. J.J. Mecholsky, S.W. Freiman and R.W. Rice, Fractographic analysis of ceramics, p.363 *in* "Fractography in Failure Analysis," A.S.T.M. Special Technical Publication 645, Philadelphia (1978).
45. J.J. Mecholsky and S.W. Freiman, Determination of fracture mechanics parameters through fractographic analysis of ceramics, p.136 *in* "Fracture Mechanics Applied to Brittle Materials," A.S.T.M. Special Technical Publication 678, Philadelphia (1979).
46. D.B. Marshall, B.R. Lawn and J.J Mecholsky, Effect of residual contact stresses on mirror/flaw-size relations, *J. Am. Ceram. Soc.* 63: 358 (1980).
47. J.J. Mecholsky, unpublished work.
48. B.T. Khuri-Yakub, A.G. Evans and G.S. Kino, Acoustic surface wave measurements of surface cracks in ceramics, *J. Am. Ceram. Soc.* 63: 65 (1980).
49. J.J.W. Tien, B.T. Khuri-Yakub, G.S. Kino, D.B. Marshall and A.G. Evans, Surface wave measurements of surface cracks in ceramics, to be published.
50. B.J. Hockey, Crack healing in brittle materials, this volume.
51. D.B. Marshall, private communication.
52. M.G. Mendiratta and J.J. Petrovic, Prediction of fracture surface energy from microhardness indentation in structural ceramics, *J. Mater. Sci.* 11: 973 (1976).
53. A.G. Evans and E.A. Charles, Fracture toughness determinations by indentation, *J. Am. Ceram. Soc.* 59: 371 (1976).
54. A.G. Evans, Fracture toughness: the role of indentation techniques, p.112 *in* "Fracture Mechanics Applied to Brittle Materials," S.W. Freiman, ed., A.S.T.M. Special Technical Publication 678, Philadelphia (1979).
55. R.H. Marion, Use of indentation fracture to determine fracture toughness, p.103 *in* "Fracture Mechanics Applied to Brittle Materials," S.W. Freiman, ed., A.S.T.M. Special Technical Publication 678, Philadelphia (1979).

56. G.R. Anstis, P. Chantikul, B.R. Lawn and D.B. Marshall, A critical evaluation of indentation techniques for measuring fracture toughness: I. Direct crack measurements, *J. Am. Ceram. Soc.*, in press.
57. P. Chantikul, G.R. Anstis, B.R. Lawn and D.B. Marshall, A critical evaluation of indentation techniques for measuring fracture toughness: II. Strength method, *J. Am. Ceram. Soc.*, in press.
58. N. Shinkai, R.C. Bradt and G.E. Rindone, The fracture toughness of fused silica and float glass at elevated temperatures, *J. Am. Ceram. Soc.*, in press.
59. S.M. Wiederhorn and J.E. Ritter, Application of fracture mechanics concepts to structural ceramics, p.202 *in* "Fracture Mechanics Applied to Brittle Materials," S.W. Freiman, ed., A.S.T.M. Special Technical Publication 678, Philadelphia (1979).
60. D.B. Marshall and B.R. Lawn, Flaw characteristics in dynamic fatigue: the influence of residual contact stresses, *J. Am. Ceram. Soc.* 63: 532 (1980).
61. P. Chantikul, B.R. Lawn and D.B. Marshall, Micromechanics of flaw growth in static fatigue: influence of residual contact stresses, *J. Am. Ceram. Soc.*, in press.
62. B.R. Lawn, D.B. Marshall, G.R. Anstis and T.P. Dabbs, Fatigue analysis of brittle materials using indentation flaws: I. General theory, *J. Mater. Sci.*, in press.
63. R.F. Cook, B.R. Lawn and G.R. Anstis, Fatigue analysis of brittle materials using indentation flaws: II. Case study on a glass-ceramic, *J. Mater. Sci.*, in press.
64. B.J. Pletka and S.M. Wiederhorn, A comparison of failure predictions by strength and fracture mechanics techniques, to be published.
65. T.P. Dabbs, B.R. Lawn and P.L. Kelly, A dynamic fatigue study of soda-lime and borosilicate glasses using small-scale indentation flaws, to be published.
66. T.P. Dabbs, D.B. Marshall and B.R. Lawn, Flaw generation by indentation in glass fibers, *J. Am. Ceram. Soc.* 63: 224 (1980).
67. T.P. Dabbs, unpublished work.
68. D.B. Marshall and B.R. Lawn, Residual stresses in dynamic fatigue of abraded glass, *Comm. Am. Ceram. Soc.* 64: C6 (1981).